Interferometric Synthetic Aperture Millimeter-wave Radiometer for the High Resolution Imaging

Yong-Hoon Kim*, Jung-Hee Choi, Gum-Sil Kang***
***Kwangju Institute of Science and Technology (K-JIST)**
1 Oryong-dong, Puk-gu, Kwangju, 500-712, Korea
Tel: +82-62-970-2387, Fax: +82-62-970-2384, E-mail: yhkim@kjist.ac.kr
**** Taegu University, 15 Naeri JinRyang, Kyungsan, Kyungpook, 712-714, Korea**

ABSTRACT

The imaging characteristics of a 2-D interferometric synthetic aperture radiometer, such as an angular resolution, depend largely on the type of an antenna array. In this paper, different array configurations of antenna are studied and compared with each array types to get more high resolution image in spatial. T-, X- and Y- types of antenna array are considered and the performances of each type are analyzed considering spatial resolution. The simulation results of candidate antenna types are presented in this paper. In case of Y-type the coverage area of the visibility function is wide and the angular resolution is high more than the others. X-type array shows the good performance for side lobe level.

I. INTRODUCTION

Airborne and spaceborne microwave radiometers have been used for the passive remote sensing of the earth's surface parameters such as sea surface temperature, salinity, windspeed and soil moisture content. Whenever a high spatial resolution is desired, the conventional real aperture radiometer requires a large size antenna and a scanning mechanism if it is necessary.

The interferometric synthetic aperture radiometer is an attractive alternative to the conventional real aperture imaging system for the passive remote sensing application. It is a most important advantage of interferometric radiometer that high angular resolution can be achieved by aperture synthesis with a static and array of small antennas, avoiding the scanning of the large antennas required by real aperture system [1].

The angular resolution of real aperture radiometer is decided by the antenna radiation pattern but for the interferometric radiometer, angular measurement depends on the configuration type of antenna array. Generally Y-type antenna array have been suggested as most efficient configuration of antenna array for a 2-D interferometric synthetic aperture radiometer because wide alias free FOV (Field Of View) and wide coverage of visibility function can be obtained [2]. In this paper several kinds of antenna array configuration are examined on the view of visibility coverage and the sampling shape and the characteristics of synthesized beam according to the configuration of antenna array are analyzed and compared through simulation results.

II. Interferometric Measurement of 2-D Image

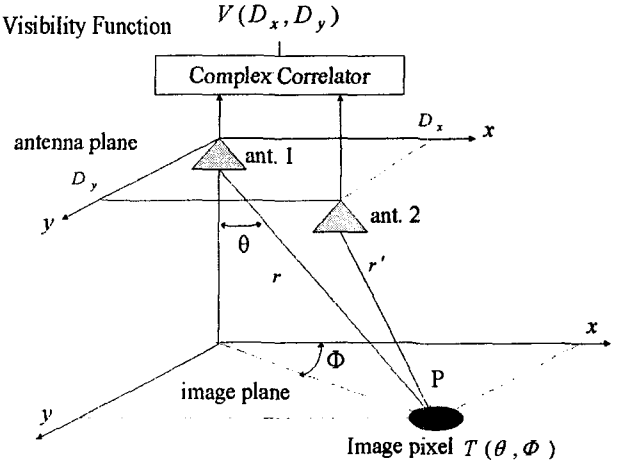

Figure 1. The geometry of interferometric measurement for synthetic aperture radiometer.

Figure 1 shows the geometry of interferometric measurement for aperture synthesis. There is a pair of

antennas on the antenna plane and it is assumed that two antennas have an overlapping FOV. D_x and D_y mean the relative distance of two antennas on the x and y axis, respectively. Interferometric measurement can be achieved by relative distance of two antennas to the image pixel P. The return signal of an image pixel on the observation area is modeled by brightness temperature $T(\theta,\phi)$ because the radiometer measures natural radiation energy of the target. The output signal of the interferometric radiometer is called by visibility function $V(D_x, D_y)$, which is obtained through the complex cross correlation of two signals collected by a pair of antennas [1]. Equation (1) and (2) show the mathematical expression of complex cross correlation output for the interferometric radiometer.

$$\mathrm{Re}[V(D_x,D_y)] = E[b_1(t)b_2(t)] = R_{b_1b_2}(\tau)\big|_{\tau=0} \quad (1)$$

$$\mathrm{Im}[V(D_x,D_y)] = E\left[b_1(t)b_2(t-\frac{1}{4f_c})\right] = R_{b_1b_2}(\tau)\big|_{\tau=0} \quad (2)$$

The correlator for interferometric radiometer measures the maximum cross correlation value of two noise like signal at time τ=0. The mathematical formulation of visibility function sampled by complex cross correlation is given by equation (3). In equation (3) the visibility function is expressed as an inverse Fourier Transform of the brightness temperature image. Therefore the brightness temperature image can be reconstructed by equation (4) from visibility functions sampled on the antenna plane through Fourier Transformation.

$$V(u,v) = \iint_{4\pi} T(\theta,\Phi)\exp[j2\pi(u\sin\theta\cos\Phi + v\sin\theta\sin\Phi)] \times\sin\theta\, d\theta\, d\Phi \quad (3)$$

where $u = \frac{D_x}{\lambda}$, $v = \frac{D_y}{\lambda}$.

$$\hat{T}_B(\zeta,\eta) = \int_{-\infty}^{\infty}\int_{-\infty}^{\infty} V(u,v)\exp[-j2\pi(u\zeta + v\eta)]\, du\, dv \quad (4)$$

where $\zeta = \sin\theta\cos\Phi$, $\eta = \sin\theta\sin\Phi$.

There are only two antennas on the antenna plane for explanation in the Figure 1 but practically, many small antennas are distributed on this plane and the visibility samples are measured at the same time.

III. IMAGE RECONSTRUCTION ACCORDING TO THE TYPE OF ANTENNA ARRAY

A. Antenna Array and Visibility Function

In equation (4) the brightness temperature image can be reconstructed under the assumption that the visibility function is sampled on the infinite region continuously. This the distributed brightness temperature image is band limited by the unit circle $\zeta^2 + \eta^2 \le 1$. That is, the FOV of estimated image is 4π Sr that covers the all of the observation area. Practically the visibility samples are measured discretely on the limited region and the brightness temperature image is estimated by discrete equation given by (5)

$$\hat{T}_B(\zeta,\eta) = \sum_m\sum_n V(u_m,v_n)\exp[-j2\pi(u_m\zeta + v_n\eta)]. \quad (5)$$

Due to the discrete measurement, the reconstructed image is suffered from alias effect. Also the angular resolution is limited by the sampling area of visibility function. In fact, the synthesized beamwidth is improved proportionally to the coverage area of visibility sample. From equation 3 the visibility function depends only on the relative distance of an antenna pair selected for complex cross correlation. Therefore the sampling characteristics and the visibility function coverage are decided by the configuration type of antenna array. Several kinds of 2-D antenna configuration such as T-, Y-, X-types can be used for the interferometric aperture synthesis of radiometer. Figure 2 shows the Y-type, T-type and X-type antenna array, and Figure 3, 4 show the sampled visibility function of each type and alias effect due to discrete measurement, respectively. In Figure 3 the visibility samples are measured on hexagonal grid for the Y-type, X-type and rectangular gird for T-type antenna array [3].

The visibility function coverage is more wide in case Y-type array and more high angular resolution than another types is expected. The alias effect for each antenna configuration depends on the shape of visibility sampling [2][3][4]. The alias free FOV is more wide in case of hexagonal sampling than rectangular grid in Figure 4.

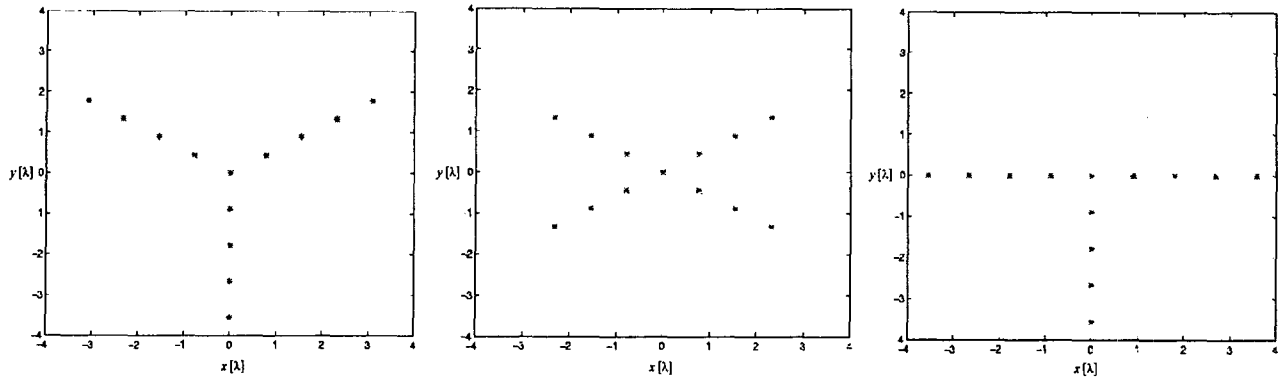

(a) Y-type (b) X-type (c) T-type

Figure 2. (a) Y-type, (b) X-type, and (c) T-type antenna array

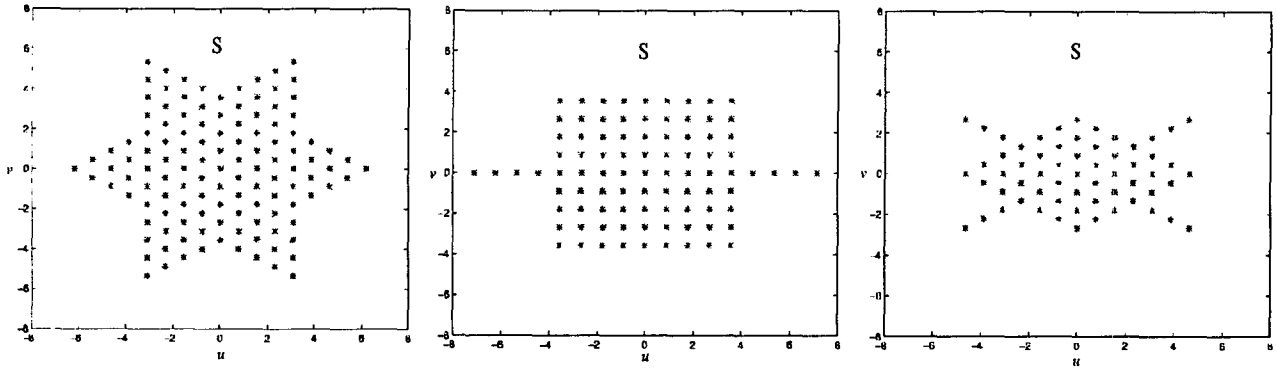

(a) Y-type configuration (b) X-type configuration (c) T-type configuration

Figure 3. Sampled visibility functions for (a) Y-type, (b) X-type, and (c) T-type configuration

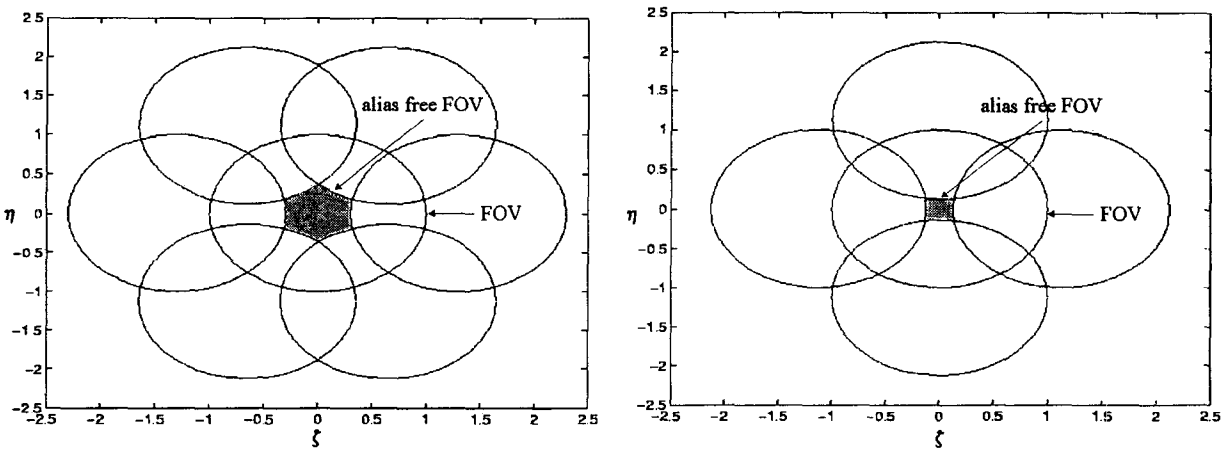

(a) Y-type and X-type configuration (b) T-type configuration

Figure 4. Alias effects for (a) Y-type and X-type and (b) T-type configuration

B. Synthesized Beamwidth

To analyze the characteristics of synthesized beam such as a beamwidth, side lobe level for interferometric radiometer, an array factor, which is equal to the impulse response, can be used [1][2]. The array factor can be computed from the relation between the original brightness temperature image and the visibility function given by equation (3) and (6). A window function *W(u,v)* is added in the image reconstruction formulation given by equation (6) because it is used to decrease the side lobe level practically when the temperature brightness image is reconstructed from the sample visibility function.

$$\hat{T}(\zeta,\eta) = \iint_S W(u,v)V(u,v)\exp[-j2\pi(u\zeta+v\eta)]\,du dv \quad (6)$$

$$= \iint_S \Big[\iint_{\zeta'^2+\eta'^2\le 1} T(\zeta',\eta')\exp\{-j2\pi(u\zeta'+v\eta')\}d\zeta' d\eta' \Big] \times W(u,v)\exp[j2\pi(u\zeta+v\eta)]\,du dv \quad (7)$$

$$= \iint_{\zeta'^2+\eta'^2\le 1} AF(\zeta,\zeta',\eta,\eta')T(\zeta',\eta')\,d\zeta' d\eta' \quad (8)$$

where the array factor

$$AF(\zeta,\zeta',\eta,\eta') = \iint_S W(u,v) \times \exp[j2\pi(u(\zeta-\zeta')+v(\eta-\eta'))]\,du dv \quad (9)$$

and $W(u,v)$ is a window function.

The array factor $AF(\zeta,\zeta',\eta,\eta')$ is expressed in equation (9), where $T(\zeta',\eta')$ means the original brightness temperature image, $\hat{T}(\zeta,\eta)$ is the estimated image at the ζ, η from $T(\zeta',\eta')$ and S indicates the coverage area of sampled visibility function. From the view of array factor, it can be said that the true brightness temperature distribution is reconstructed by the array factor at every position.

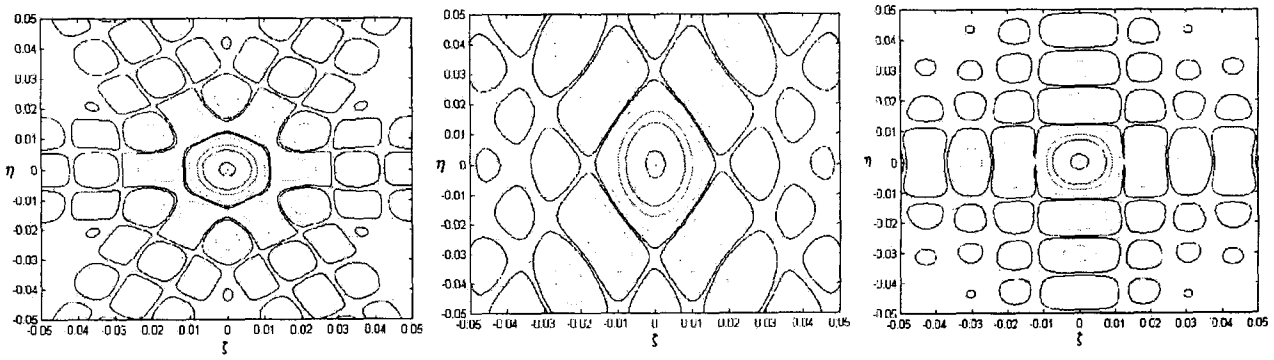

(a) Y-type (b) X-type (c) T-type

Figure 5. 2-D array factor for (a) Y-type, (b) X-type, and (c) T-type array configuration

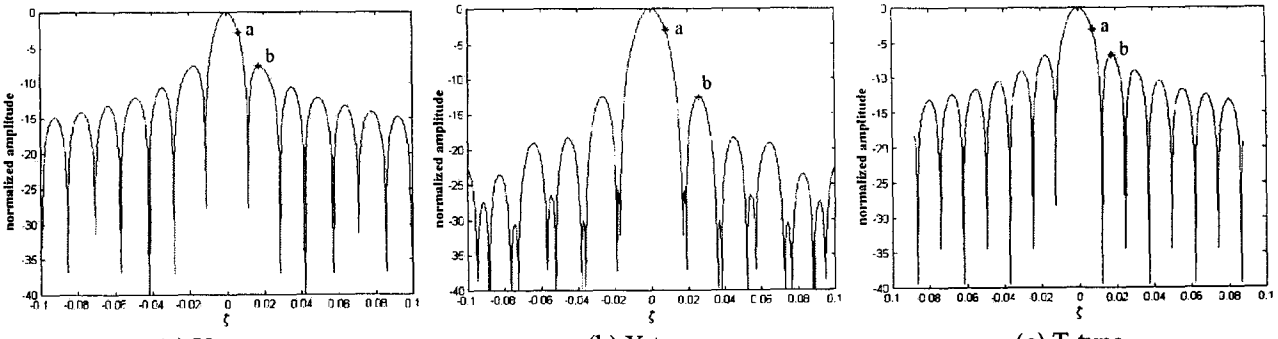

(a) Y-type (b) X-type (c) T-type

Figure 6.1-D array factor for (a) Y-type, (b) X-type, and (c) T-type array configuration

Figure 5 show the simulated 2-D array factors for Y-type, X-type and T-type configurations. For computation of 2-D array factor, the total antenna elements of 136 is used for each type. The relative distance of adjacent antenna elements is 0.89 λ in the all of the antenna array and the rectangular window function is used for image reconstruction. In Figure 5 each 2-D array factors have the particular figure due to the different shape of visibility sample coverage for three types of array configurations. The angular resolution of synthesized beam is considered as a 3 dB beamwidth of array factor in this paper. The angular resolution and the side lobe level for each configuration can be founded from 1-D array factor presented in Figure 6. In Figure 6 'a' and 'b' indicate the 3 dB point and side lobe level, respectively. The angular resolution for Y-type array is better than other type and this characteristic can be predicted from the area of the visibility coverage. The side lobe level of X-type is the lowest among three types. The 3 dB synthesized beamwidth and side lobe level for each types of configuration are given by Table 1.

Table 1. The characteristics of synthesized beam according to the type of antenna array

	The type of antenna array		
	Y-type	X-type	T-type
3 dB beamwidth ($\Delta\zeta$)	0.013	0.016	0.0148
Side lobe level (dB]	-7.6240	-12.51	-6.7497

IV. CONCLUSION

In this paper, the characteristics of interferometric synthesized beam are examined according to the kinds of array configuration Y-type, X-type and T-type using the array factor. The 2-D array factors for each configurations are computed through the simulation and the angular resolution and side lobe level are examined. For angular resolution, Y-type configuration is efficient method because the visibility functions are measured on wide coverage and the more high angular resolution can be achieved more than the other types. For the side lobe level, X-type array shows the better performance than the Y- and T-types.

ACKNOWLEDGEMENT

This work was supported in part by the Korea Science and Engineering Foundation (KOSEF) through the Advanced Environmental Monitoring Research Center at Kwangju Institute of Science and Technology.

REFERENCE

[1] CHRISTOPER S. RUF, CALVIN T. SWIFT, ALAN B. TANNER 1988. Interferometric Synthetic Aperture Microwave Radiometry for the Remote Sensing of the Earth, *IEEE Transactions on geoscience and remote sensing, Vol. 26, No. 5*, pp. 597-611.

[2] J. Bara, A. Camps, 1998. Angular resolution of two-dimensional, hexagonally sampled interferometric radiometers, *Radio Science, Vol. 33, Number 5, September-October, pp. 1459-1473.*

[3] James C. Ehrhardt, 1993. Hexagonal Fast Fourier Transform with Rectangular Output, *IEEE Transactions on signal processing, Vol. 41, No. 3, MARCH, pp. 1469-1472.*

[4] RUSSELL M. MERSEREAU, 1979. The Processing of Hexagonally Sampled Two-Dimensional Signals, *Proceeding of the IEEE, Vol. 67, No. 6, JUNE, pp.930-949.*